Chaotic dynamics of a swirling flame front instability generated by a change in gravitational orientation

Hiroshi Gotoda* and Hiroaki Kobayashi
Department of Mechanical Engineering, Tokyo University of Science, 6-3-1 Niijuku, Katsushika-ku, Tokyo 125-8585, Japan

Kenta Hayashi
Department of Mechanical Engineering, Ritsumeikan University, 1-1-1 Nojihigashi, Kusatsu, Shiga 525-8577, Japan
(Received 18 August 2016; revised manuscript received 11 November 2016; published 1 February 2017)

We have intensively examined the dynamic behavior of flame front instability in a lean swirling premixed flame generated by a change in gravitational orientation [H. Gotoda, T. Miyano, and I. G. Shepherd, Phys. Rev. E **81**, 026211 (2010)] from the viewpoints of complex networks, symbolic dynamics, and statistical complexity. Here, we considered the permutation entropy in combination with the surrogate data method, the permutation spectrum test, and the multiscale complexity-entropy causality plane incorporating a scale-dependent approach, none of which have been considered in the study of flame front instabilities. Our results clearly show the possible presence of chaos in flame front dynamics induced by the coupling of swirl-buoyancy interaction in inverted gravity. The flame front dynamics also possesses a scale-free structure, which is reasonably shown by the probability distribution of the degree in ϵ-recurrence networks.

DOI: 10.1103/PhysRevE.95.022201

I. INTRODUCTION

The identification of chaos from time series data is an important and challenging topic in current nonlinear physics and many related disciplines of science and engineering. Nonlinear time series analysis based on dynamical systems theory has made it possible to distill the determinism inherent in complex phenomena [1]. Recent progress in the methodologies of nonlinear time series analysis has yielded significant success in obtaining an overarching understanding of nonlinear dynamics [2]. The promising usefulness of dynamical systems theory has been underscored by one of the authors in theoretical and numerical studies on a variety of hydrodynamic systems involving magnetohydrodynamic natural convection [3] and traveling waves in a falling film flow [4]. The emergence of periodic and chaotic dynamics in flame front instabilities arising from the mutual coupling of hydrodynamic, heat, and mass diffusion processes through a rapid chemical reaction is a major subject in combustion physics research. It is widely recognized that the buoyant force driven by natural convection under terrestrial gravity constitutes one of the predominant causes responsible for the generation and growth of flame front instabilities. Gotoda *et al.* [5] have recently studied the dynamic behavior of flame front instability in a lean swirling premixed flame induced by a buoyancy-swirl interaction due to a change in the gravitational direction relative to the flame front. They reported that the unstable hot combustion products generated by the hydrodynamic instability related to the Rayleigh-Taylor instability mechanism give rise to chaotic behavior of the flame front instability. An analytical method based on orbital instability, which estimates the degree of divergence of nearby trajectories in the phase space, has been adopted for the characterization of the dynamical behavior, in addition to nonlinear forecasting, which can extract the short-term predictability nature. Nonlinear dynamics of flame front instabilities has been studied to some extent in the previous work [5], but more detailed and plausible analyses from different viewpoints should be taken into account to show the possible presence of chaos.

The main purpose of this work is to conduct a more plausible study of the nonlinear dynamics in flame front instability in a lean swirling premixed flame generated by a change in gravitational orientation from the viewpoints of symbolic dynamics and statistical complexity. We use two analytical methods based on symbolic dynamics: the permutation entropy [6], which allows us to evaluate the degree of randomness estimated from rank order patterns in the values of observed time series, and the permutation spectrum test [7] as an extended version of Bandt and Pompe's method [6] to distinguish chaos from stochastic dynamics. The permutation entropy represents the Shannon entropy considering the probability distribution of possible existing rank order patterns in a time series. These methods have been proactively adopted to study combustion dynamics in a thermoacoustic combustion system [8,9]. We use the multiscale complexity-entropy causality plane incorporating a scale-dependent approach [10] in terms of statistical complexity. This approach can quantify not only the randomness of dynamics but also the degree of correlational structures [11] and has also been shown to ensure good performance in distinguishing chaos from stochastic dynamics. On the other hand, time series analysis based on complex network theory is a rapidly growing research area in an increasing number of fields in nonlinear physics. It quantifies the properties in complex topologies composed of vertices and edges constructed from time series. Thus far, many methodologies for the construction of networks have been proposed such as visibility graphs [12,13], cycle networks [14], correlation networks [15], and recurrence networks [16–18]. A scale-free structure, which is shown by the presence of a power-law in the degree distribution, is a well-known important property of networks. Two experimental studies on the scale-free structure have been reported for confined turbulent combustion systems: one was on combustion noise

*gotoda@rs.tus.ac.jp

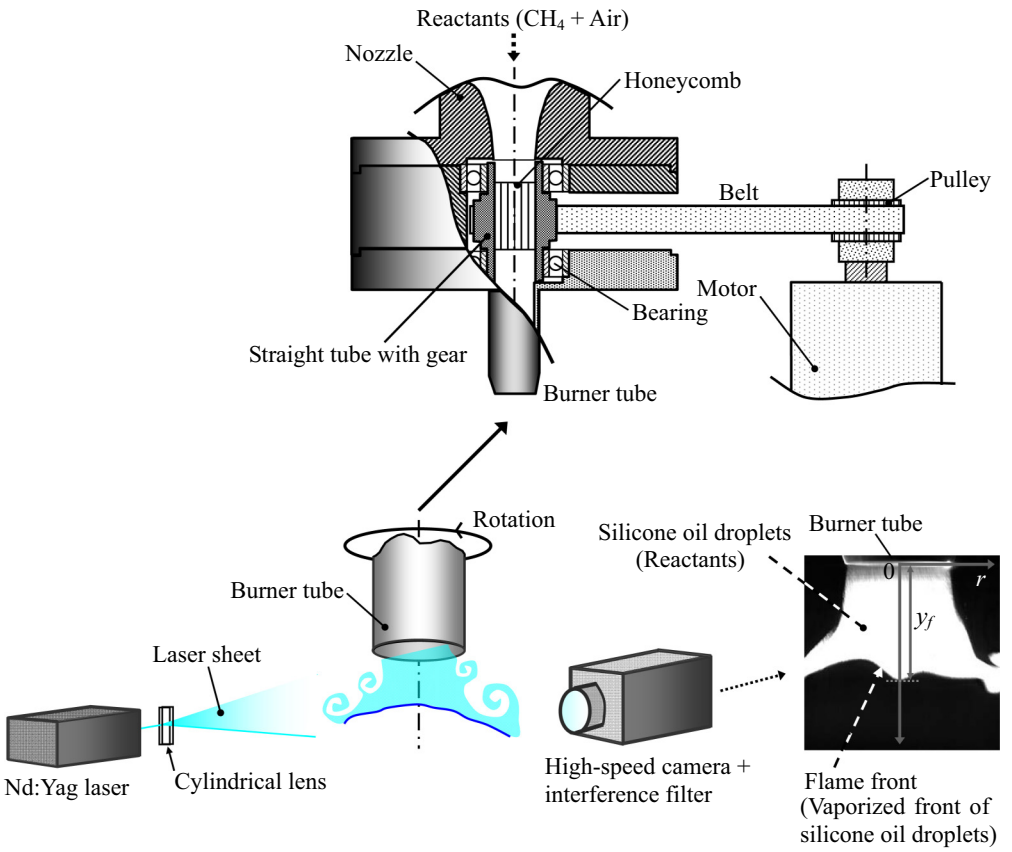

FIG. 1. Experimental system.

by estimating the degree distribution in a natural visibility graph [19], and the other was on thermoacoustic combustion oscillations by estimating the vertex strength distribution in cycle networks [20]. However, the scale-free structure has not been explored in networks constructed from flame front fluctuations induced by buoyancy-swirl coupling. Recurrence plots in phase space based on dynamical systems theory are useful for extracting the order and disorder patterns hidden in combustion dynamics [21–23]. In this sense, we examine the possible existence of a scale-free structure using the ϵ-recurrence networks proposed by Donner *et al.* [18]. In relation to the randomness of nonlinear dynamics, we also propose a network entropy considering the probability distribution of the degree in ϵ-recurrence networks. This paper is organized as follows. The experimental system and conditions are described in Sec. II. The framework for nonlinear time series analysis is described in Sec. III. We present and discuss the results in Sec. IV, and conclusions are provided in Sec. V.

II. EXPERIMENTAL SYSTEM AND CONDITIONS

Details of our experimental system have been reported in a previous work [5]. The burner system we employed in this study comprises three main parts: a diffuser, a nozzle, and a burner tube with a diameter of 12 mm. The premixed methane-air reactants are supplied to the diffuser. As shown in Fig. 1, the burner tube is supported by two bearings and rotated by a DC motor through a pulley and belt system. It induces the solid-body rotation of the premixture at the burner tube exit. We set the mean flow velocity of the reactants U (= volume flow rate/cross-sectional area of the burner tube) from 0.8 m/s (buoyancy-dominated regime: $R_i > 0.1$) to 1.6 m/s (momentum-dominated regime: $R_i < 0.1$), where R_i is the Richardson number [24,25]. In this study, the equivalence ratio and the swirl number of the reactants are varied from 0.70 to 0.75 and 0.65 to 0.76, respectively, because it is under these conditions that flame front instability is clearly formed. Similarly to the previous study [5], the flame front is extracted by a laser tomographic method with a high-speed camera (Photron 1024 PCI, Japan). The Mie scattered light emitted from the dispersed silicone oil droplets in the reactants shows the region where the temperature is below ~570 K; this region corresponds to the upstream side of the preheat zone [26]. The spatial resolution of the visualized images is 27 pixels/mm, which is sufficient for dealing with the flame front dynamics. Similarly to the previous study [5], the location of the flame front along the centerline of the burner tube is defined as the flame front location y_f(mm), and the deviation from the mean flame front location $\Delta y_f = y_f - \bar{y}_f$ (where $\bar{y}_f$ is the time-averaged flame front location as a function of time t) is obtained as a function of time. Time series analyses involving the degree and network entropy in ϵ-recurrence networks, the permutation entropy in combination with the surrogate data method, the permutation spectrum test, and the multiscale complexity-entropy causality plane (CECP) are adopted for the temporal evolution of Δy_f.

III. NONLINEAR TIME SERIES ANALYSIS

We compute the permutation entropy of flame front fluctuations in a manner similar to in Ref. [8]. We first index all possible permutations ($D!$ permutations) of D successive data points in a time series as π, where D is the embedding dimension. After counting the relative frequency of each permutation pattern $p(\pi)$ for all vectors $\Delta\mathbf{y}_f(t)(=(\Delta y_f(t),\Delta y_f(t+\tau),\ldots,(t+(D-1)\tau))$, we estimate the permutation entropy H_p normalized by the maximum permutation entropy ($=\log_2 D!$) corresponding to completely random processes as follows:

$$H_p = \frac{-\sum_\pi p(\pi)\log_2 p(\pi)}{\log_2 D!}. \tag{1}$$

Here, H_p is zero for a monotonically increasing or decreasing process and unity for a completely random process. In this study, we adopt the surrogate data method considering the null hypothesis that the irregular components of flame front fluctuations are governed by a linear stochastic process with a nonlinear observation function. Under this null hypothesis, we generate surrogate time series data with the same probability density functions and power spectra as those of the original time series using the iterative amplitude-adjusted Fourier transform (IAAFT) surrogate method [27–32]. Statistics such as the mean and variance, and the power spectral structure of the original time series are preserved in the surrogate time series. Note that the number of iterations is set to 10 in this study to reduce the false rejection rate [27]. We reject the null hypothesis if the difference between the values of H_p estimated for the original and surrogate time series data is sufficiently large. We perform the permutation spectrum test [7] to test for nonlinear determinism underlying complex dynamics. The permutation spectrum consists of the relative frequency distribution of permutation patterns for disjointed windows of length L ($=200$ ms), into which Δy_f is partitioned, and their standard deviation between the windows. The important point in this method is that the appearance of zero standard deviation with some forbidden patterns (original patterns that do not exist in the frequency distribution) suggests the presence of nonlinear deterministic dynamics.

The CECP, which is obtained by plotting the Jensen-Shannon statistical complexity against the permutation entropy, is useful for quantifying the complexity of nonlinear dynamics [11]. It has recently been adopted for the analysis of turbulence in laboratory plasmas and solar wind [33]. We consider the multiscale CECP [10] incorporating the variations in the time delay of the phase space to identify the possible presence of chaos:

$$C_{JS}[\mathbf{P}] = Q_{JS}[\mathbf{P},\mathbf{P}_e]H_p[\mathbf{P}], \tag{2}$$

$$Q_{JS}[\mathbf{P},\mathbf{P}_e] = \frac{\log_2 D!}{Q_{JS,\max}}\{H_p[(\mathbf{P}+\mathbf{P}_e)/2] - H_p[\mathbf{P}]/2 - H_p[\mathbf{P}_e]/2\}. \tag{3}$$

Here, C_{JS} is the Jensen-Shannon statistical complexity, H_p is the permutation entropy, Q_{JS} is the disequilibrium, $\mathbf{P}_e$ is the uniform distribution corresponding to a completely random process ($=\{1/D!,\ldots,1/D!\}$), and $Q_{JS,\max}$ is the maximum possible value of $Q_{JS}[\mathbf{P},\mathbf{P}_e]$. $Q_{JS,\max}$ can be described by Eq. (4) when one of the components of $\mathbf{P}$ is unity and the other components are zero. C_{JS} can take values between a minimum of $C_{JS,\min}$ and maximum of $C_{JS,\max}$ in terms of H_p:

$$Q_{JS,\max} = -\frac{1}{2}\left\{\frac{D!+1}{D!}\log_2(D!+1) - 2\log_2(2D!) + \log_2(D!)\right\}. \tag{4}$$

In this study, we apply ϵ-recurrence networks [18] to flame front fluctuations. They are represented by its adjacency matrix $\mathbf{A}$ consisting of $A_{ij} = \Theta[\epsilon - \|\Delta\mathbf{y}_f(t_i) - \Delta\mathbf{y}_f(t_j)\|] - \delta_{ij}$, where Θ is the Heaviside function, δ_{ij} is the Kronecker delta, and ϵ is a threshold. We set the value of ϵ so as to satisfy an edge density $\leqslant 0.05$ [34,35]. The value of the embedding delay time τ, at which the mutual information first reaches a minimum, or τ that reduces the mutual information to below e^{-1}, is used to construct the networks in accordance with the prescription of Fraser and Swinney [36].

IV. RESULTS AND DISCUSSION

Variations in H_p as a function of D are shown in Fig. 2 for the original time series and 20 sets of IAAFT surrogate time series at $U = 1.0$ m/s. Note that, similarly to in a previous study reported by Bandt and Pompe [6], τ is set to 1. H_p for the original time series data gradually decreases with increasing D. We observe a similar trend for H_p in terms of D for the IAAFT surrogate time series data. The important point here is that the estimates of H_p for the original time series data are conspicuously lower than those for the surrogate time series data at each embedding dimension, indicating a significant inconsistency between them. In fact, we can reject the null hypothesis by performing a two-sided t-test on the estimated H_p at 5% reliability, which indicates that highly visible determinism relevant to rank order patterns is present in the flame front dynamics. The Lorenz system, derived by considering three low-ordered modes in the truncated Fourier expansions of the stream

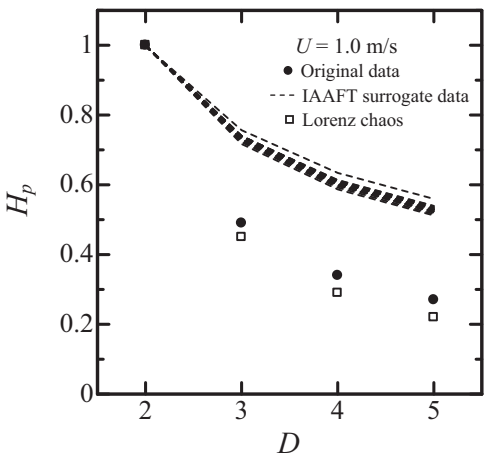

FIG. 2. Variations in permutation entropy H_p of flame front fluctuations Δy_f as a function of embedding dimension D: original data (•), IAAFT surrogate data (lines) at mean flow velocity of the reactants of $U = 1.0$ m/s, and Lorenz chaos (□).

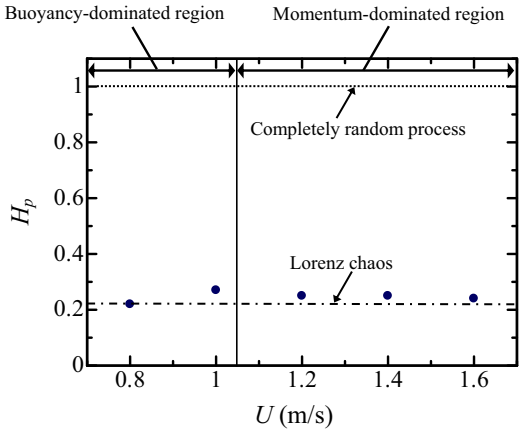

FIG. 3. Variations in permutation entropy H_p of flame front fluctuations Δy_f as a function of mean flow velocity of the reactants U. The embedding dimension D and the embedding delay time τ are 5 and 1, respectively.

function and the temperature from the Oberbeck-Boussinesq equations, can give rise to deterministic chaos. However, it is an oversimplified low-dimensional deterministic system and is not appropriate as a platform for describing flame front instability. Nevertheless, it is useful for the purpose of our study because it enables us to discuss the degree of randomness of dynamic behavior in unstable phenomena generated by buoyancy-driven hydrodynamic instabilities. As shown in Fig. 2, H_p for the original time series at each D takes slightly higher values than that of low-dimensional chaos (the normalized Rayleigh number r is 28) produced by the Lorenz system. That is, the dynamic behavior of unstable flame front fluctuations has a slightly higher degree of randomness than low-dimensional deterministic chaos. Figure 3 shows H_p estimated from the original time series data at $D = 5$ and $\tau = 1$ as a function of U. H_p remains approximately unchanged with increasing U. Determinism governing the flame front fluctuations in the buoyancy-dominated region persists even in the momentum-dominated region. This corresponds to the results for the translation error [5].

Figure 4 shows the frequency distribution of the permutation patterns for each window and their standard deviation between the windows at $U = 1.0$ m/s. We clearly observe zero standard deviation with some forbidden patterns. According to the findings reported by Kulp and Zunino [7], the dynamic behavior of unstable flame front fluctuations represents chaos. Variations in the number of forbidden patterns N_f normalized by the maximum number of possible forbidden patterns ($= D!$) are shown in Fig. 5 as a function of U. N_f takes a lower value at $U = 1.0$ m/s than that in the case of Lorenz chaos. This means that the degree of nonlinear determinism is lower than that of Lorenz chaos, which reasonably corresponds to the result obtained from the permutation entropy (Fig. 3). The interesting result here is that N_f remains nearly unchanged in terms of U, which clearly shows that the same degree of nonlinear determinism as that for the buoyancy-dominated region persists even in the momentum-dominated region.

A recent theoretical study [37] on low-dimensional systems has reported that the network entropy in ϵ-recurrence networks

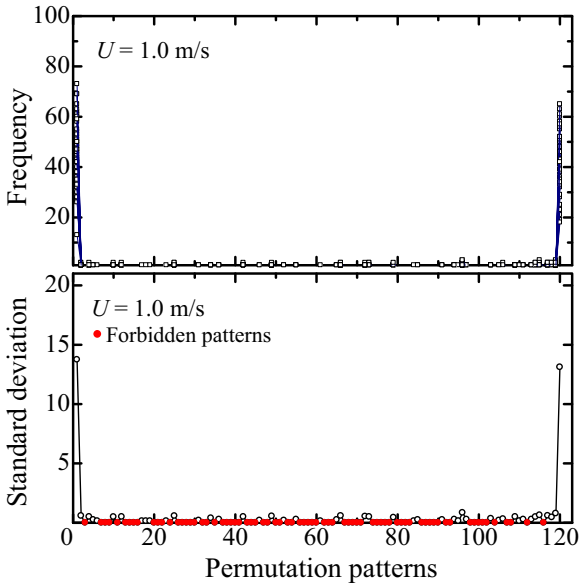

FIG. 4. Frequency distribution of permutation patterns of flame front fluctuations Δy_f for each window and their standard deviation between the windows at mean flow velocity of the reactants of $U = 1.0$ m/s. The embedding dimension D and the embedding delay time τ are 5 and 1, respectively. Forbidden patterns are shown as red plots.

captures the significant transition to chaos via the period-doubling bifurcation process. In this study, we estimate the network entropy H_n defined as

$$H_n = -\sum_k P(k) \ln P(k). \tag{5}$$

Here, k is the degree and $P(k)$ is the existing probability distribution of k in the ϵ-recurrence networks. Variations in H_n as a function of U are shown in Fig. 6. H_n remains nearly unchanged with increasing U. It takes a value slightly higher than that of low-dimensional chaos produced by the

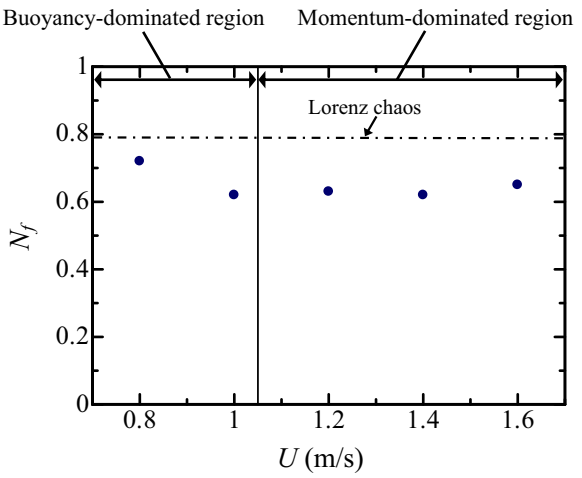

FIG. 5. Variations in the number of forbidden patterns N_f normalized by the maximum number of possible forbidden patterns ($= D!$) as a function of mean flow velocity of the reactants U at the embedding dimension $D = 5$ and the embedding delay time $\tau = 1$.

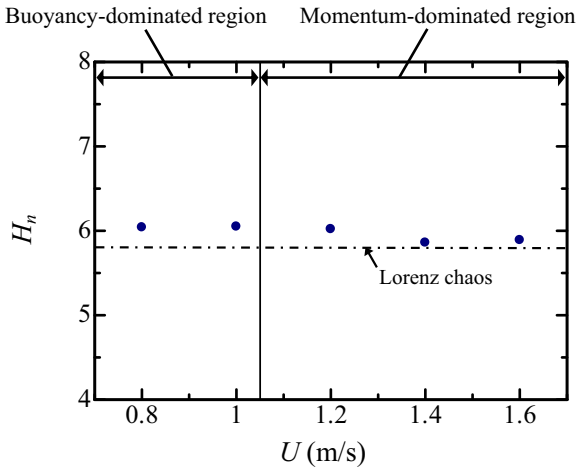

FIG. 6. Variations in the network entropy H_n as a function of mean flow velocity of the reactants U at the embedding dimension $D = 5$. Note that the embedding delay time τ for different U is determined by the mutual information in accordance with the prescription of Fraser and Swinney [36].

Lorenz system. This means that flame front dynamics has a slightly higher degree of randomness than low-dimensional deterministic chaos, which corresponds to the results obtained from the permutation entropy and the number of forbidden patterns. This result also clearly shows that the network entropy considering the probability distribution of the degree in ϵ-recurrence networks is valid for dealing with flame front instabilities. Figure 7 shows the probability distribution of the degree k in the networks at $U = 1.6$ m/s as a representative case. It exhibits power-law decay, although the plots appear to be scattered. The scaling exponent is inferred to be -3.3, indicating the possible presence of a scale-free structure. This

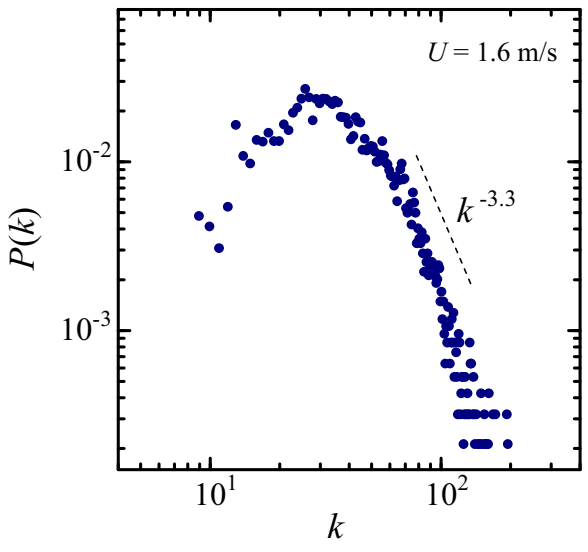

FIG. 7. Probability distribution of the degree $P(k)$ in the ϵ-recurrence networks at mean flow velocity of the reactants of $U = 1.6$ m/s. The embedding dimension D and the embedding delay time τ are 5 and 100, respectively.

gives the finding that the flame front dynamics possesses the scale invariance associated with fractality.

Variations in H_p and C_{JS} of Δy_f in terms of the embedding delay time τ at $U = 1.0$ m/s are shown in Fig. 8, together with the CECP involving $C_{JS,\min}$ and $C_{JS,\max}$. H_p monotonically increases with increasing τ up to 40 and finally becomes nearly constant. In contrast, C_{JS} has a maximum value at $\tau = 9$ and gradually decays with increasing τ. A similar trend toward chaos was reported by Zunino *et al.* [10]. The location of (H_p, C_{JS}) moves from left to right in the CECP with increasing τ. The trajectory on the CECP reasonably corresponds to that of Lorenz chaos [38]. Similar results are observed for $U = 1.6$ m/s, corresponding to the momentum-dominated region. This gives us sufficient evidence of the presence of low-dimensional chaos in flame front instability. In this study, we also investigate the variations in H_p and C_{JS} in terms of τ at $U = 1.6$ m/s, together with the CECP for the interface fluctuations Δy_i between combustion products and the surrounding air, with the aim of obtaining a more comprehensive understanding of flame front dynamics. Note that $\Delta y_i = y_i - \bar{y}_i$, where Δy_i is the deviation from the mean combustion products/surrounding air interface location and y_i is the time-averaged interface location as a function of time [5]. As shown in Fig. 9, the profiles of H_p and C_{JS} in terms of τ and the trajectory on the CECP clearly show the presence of low-dimensional chaos in the interface fluctuations. On the basis of a previous study [5], it is conceivable that flow fluctuations induced by unstable vortex breakdown due to a buoyancy-swirl interaction have a significant effect on the chaotic behavior of unstable flame front fluctuations.

It has been pointed out by Cencini *et al.* [39] that chaotic features of dynamics in a system are mainly dependent on the time resolution of the obtained time series. This means that the estimation of nonlinear invariants over a wide range of time scales incorporating a scale-dependent approach should be taken into account to discuss whether or not nonlinear determinism is intrinsically present in the underlying dynamics. In this sense, the multiscale CECP involving the changes in the embedding delay time has recently been applied to an experimental study on nonlinear dynamics in vertical wind velocity fluctuations in a turbulent atmospheric surface layer [40]. A substantial number of experimental and theoretical studies on nonlinear dynamics in various types of combustion dynamics involving a thermal pulse combustor [41–43], a thermoacoustic combustion system [8,9,22,44–50], a spark ignition engine [51–53], a diesel engine [54], and detonation [55–57] have adopted nonlinear time series analysis on the basis of dynamical systems theory to extract the chaotic features in a system, but this remains an open question for flame front instabilities. In addition, the scale-dependent approach to dealing with nonlinear dynamics at multiple temporal scales was not adopted in the above studies [8,9,22,41–57], and a specific embedding delay time determined by mutual information in accordance with the prescription of Fraser and Swinney [36] was only considered to estimate nonlinear invariants of the dynamic behavior. An important merit of using the multiscale CECP is the distinction between nonlinear deterministic and stochastic processes without the need to optimize the embedding delay time in the phase space. The

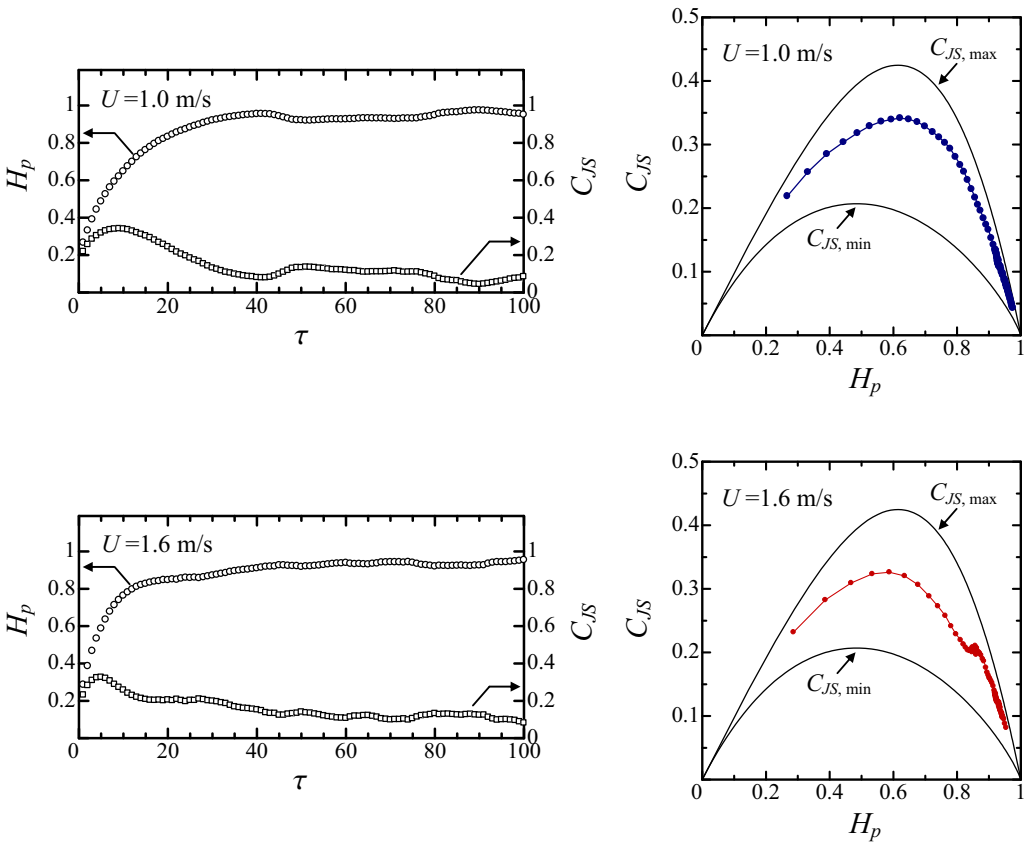

FIG. 8. Variations in permutation entropy H_p and Jensen-Shannon statistical complexity C_{JS} of flame front fluctuations Δy_f in terms of the embedding delay time τ at mean flow velocities of the reactants of $U = 1.0$ and 1.6 m/s, together with the complexity-entropy causality plane involving $C_{JS,\min}$ and $C_{JS,\max}$. The embedding dimension D is 5.

conventional approach without considering multiple temporal scales remains valid for distinguishing between two processes, but the multiscale CECP is advantageous for the treatment of flame front instability issues.

As reported in a previous study [5], as the outward centrifugal force produced by the swirl competes with the flow field in the combustion products, a large-scale toroidal vortex becomes unstable, which gives rise to fluctuations of the products-air interface. We have proposed a physical mechanism in which the flow fluctuations in the combustion products generated by the vortex motion affect the unstable stratification of the flame front (dense reactants above light combustion products) in inverted gravity. To provide additional insight into the flame front dynamics generated by the above mechanism, the temporal evolutions of the products/air interface fluctuations Δy_i and the trajectories in three-dimensional phase space $(\Delta y_i(t), \Delta y_i(t+\tau), \Delta y_i(t+2\tau))$ at $U = 1.6$ m/s are shown in Fig. 10. The six images in the first row show the combustion

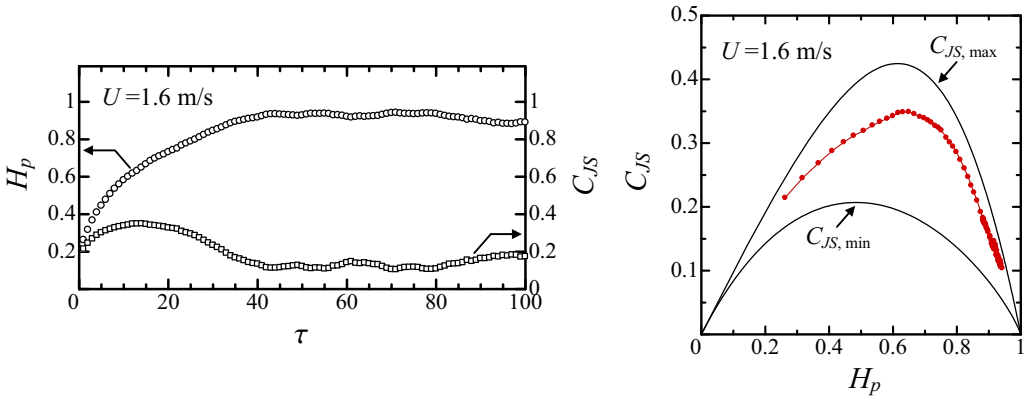

FIG. 9. Variations in permutation entropy H_p and Jensen-Shannon statistical complexity C_{JS} of interface fluctuations Δy_i between combustion products and the surrounding air in terms of the embedding delay time τ at mean flow velocity of the reactants of $U = 1.6$ m/s, together with the complexity-entropy causality plane involving $C_{JS,\min}$ and $C_{JS,\max}$. The embedding dimension D is 5.

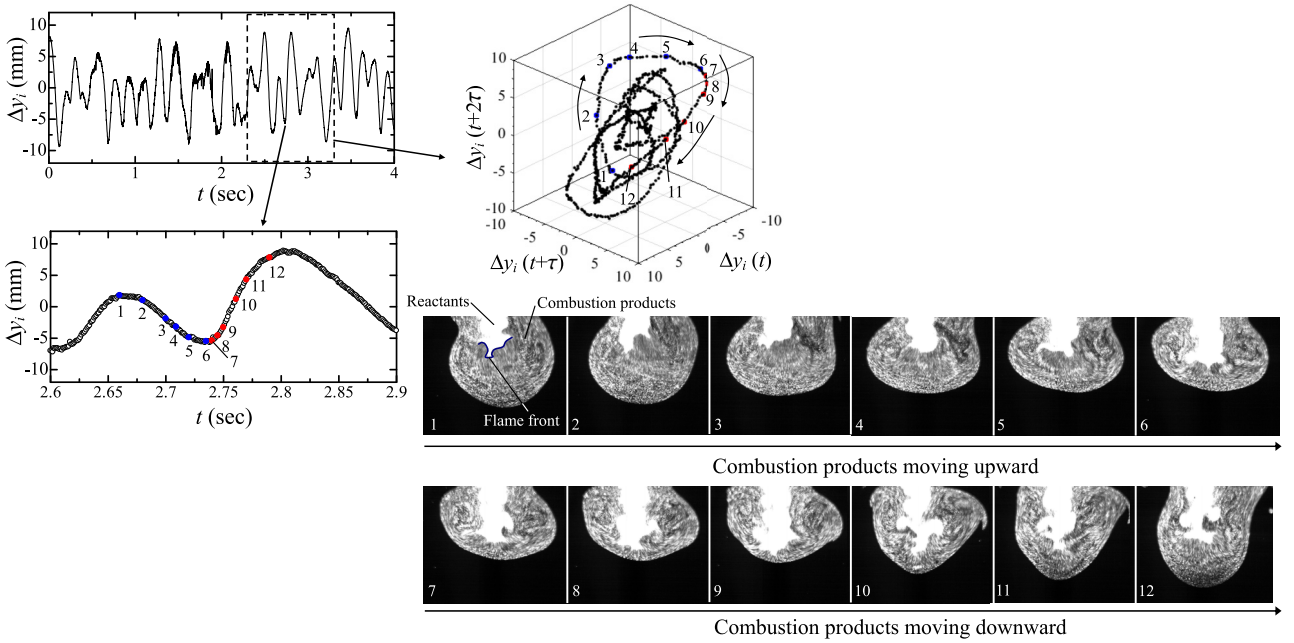

FIG. 10. Temporal evolutions of the products/air interface fluctuations Δy_i and the trajectories in three-dimensional phase space ($\Delta y_i(t)$, $\Delta y_i(t+\tau)$, $\Delta y_i(t+2\tau)$) at mean flow velocity of the reactants of $U = 1.6$ m/s.

products moving upward, while the six images in the second row show them moving downward during one cycle of the fluctuations. Points 1 and 6 in the phase space correspond, respectively, to two points near the local maximal and minimal values of Δy_i. We clearly observe the unstable deformation of flame configuration with a thick layer of combustion products (see image 1). As shown in images 2 to 5, the thickness decreases with time, maintaining the unstable front configuration, and the flame front in image 6 is further from the burner tube exit than in images 1 to 5. Bedat and Cheng [25] reported that in inverted gravity, the ratio of buoyant force to convective momentum force along the center of a burner tube increases with increasing thickness of the layer of combustion products. On this basis, the flame front begins to move downward owing to the convective momentum force overwhelming the upward buoyant force, resulting in the increase in the flame front location at point 6 in the phase space. The flame front moves downward with time in synchronization with the interface motion. However, as shown in image 10, it suddenly propagates upward, and the thickness of the layer of combustion products is significantly increased at point 12 in the phase space. This cyclic process plays an important role in low-dimensional chaotic dynamics in flame front instability induced by buoyancy-swirl coupling. In this study, we provided a physical interpretation of low-dimensional chaotic dynamics in flame front instability based on flow visualization by a laser tomographic method using TiO_2 particles as a scattering tracer. However, a high-repetition-rate OH planar laser-induced fluorescence (OH-PLIF) measurement to closely examine the simultaneous extraction of the flame front and the products-air interface should be conducted in our next study to discuss the synchronization process between the flame front and the interface fluctuations in more detail. In this work, we focused on revealing the nonlinear nature of the flame front instability. We demonstrated the possible presence of low-dimensional chaos in the flame front instability generated by a change in gravitational orientation in terms of symbolic dynamics and statistical complexity, which is a first in the area of combustion science and physics.

V. CONCLUSIONS

We have intensively examined the dynamic behavior of flame front instability in a lean swirling premixed flame generated by a change in gravitational orientation [5] in terms of complex networks, symbolic dynamics, and statistical complexity. The permutation entropy in combination with the surrogate data method, the permutation spectrum test, and the multiscale complexity-entropy causality plane (CECP) incorporating a scale-dependent approach, which quantifies both the randomness and the degree of correlational structures, provide strong evidence of the presence of low-dimensional chaos in flame front dynamics. The network entropy we proposed in this study, which considers the probability distribution of the degree in ϵ-recurrence networks, shows a similar trend to those obtained from the permutation entropy and the number of forbidden patterns, indicating that the network entropy is valid for dealing with flame front instabilities. Power-law decay of the degree distribution appears in the network, indicating the possible presence of a scale-free structure. This result shows that the flame front dynamics possesses the scale invariance associated with fractality.

ACKNOWLEDGMENT

H.G. was partially supported by the Iwatani Naoji Foundation and a Grant-in-Aid for Scientific Research (B).

[1] H. Kantz and T. Schreiber, *Nonlinear Time Series Analysis* (Cambridge University Press, Cambridge, 1997).

[2] M. Small, *Applied Nonlinear Time Series Analysis* (World Scientific, Singapore, 2005).

[3] H. Gotoda, R. Takeuchi, Y. Okuno, and T. Miyano, J. Appl. Phys. **113**, 124902 (2013).

[4] H. Gotoda, M. Pradas, and S. Kalliadasis, Intl. J. Bifurcat. Chaos **25**, 1530015 (2015).

[5] H. Gotoda, T. Miyano, and I. G. Shepherd, Phys. Rev. E **81**, 026211 (2010).

[6] C. Bandt and B. Pompe, Phys. Rev. Lett. **88**, 174102 (2002).

[7] C. W. Kulp and L. Zunino, Chaos **24**, 033116 (2014).

[8] H. Gotoda, M. Amano, T. Miyano, T. Ikawa, K. Maki, and S. Tachibana, Chaos **22**, 043128 (2012).

[9] J. Tony, E. A. Gopalakrishnan, E. Sreelekha, and R. I. Sujith, Phys. Rev. E **92**, 062902 (2015).

[10] L. Zunino, M. C. Soriano, and O. A. Rosso, Phys. Rev. E **86**, 046210 (2012).

[11] O. A. Rosso, H. A. Larrondo, M. T. Martin, A. Plastino, and M. A. Fuentes, Phys. Rev. Lett. **99**, 154102 (2007).

[12] L. Lacasa, B. Luque, F. Ballesteros, J. Luque, and J. C. Nuno, Proc. Natl. Acad. Sci. USA **105**, 4972 (2008).

[13] B. Luque, L. Lacasa, F. Ballesteros, and J. Luque, Phys. Rev. E **80**, 046103 (2009).

[14] J. Zhang and M. Small, Phys. Rev. Lett. **96**, 238701 (2006).

[15] Y. Yang and H. Yang, Physica A **387**, 1381 (2008).

[16] X. Xu, J. Zhang, and M. Small, Proc. Natl. Acad. Sci. USA **105**, 19601 (2008).

[17] Z. Gao and N. Jin, Chaos **19**, 033137 (2009).

[18] R. V. Donner, M. Small, J. F. Donges, N. Marwan, Y. Zou, R. Xiang, and J. Kurths, Intl. J. Bifurcat. Chaos **21**, 1019 (2011).

[19] M. Murugesan and R. I. Sujith, J. Fluid Mech. **772**, 225 (2015).

[20] Y. Okuno, M. Small, and H. Gotoda, Chaos **25**, 043107 (2015).

[21] L. Kabiraj and R. I. Sujith, J. Fluid Mech. **713**, 376 (2012).

[22] V. Nair, G. Thampi, and R. I. Sujith, J. Fluid Mech. **756**, 470 (2014).

[23] L. Christodoulou, L. Kabiraj, A. Saurabh, and N. Karimi, Chaos **26**, 013110 (2016).

[24] L. W. Kostiuk and R. K. Cheng, Combust. Flame **103**, 27 (1995).

[25] B. Bedat and R. K. Cheng, Combust. Flame **107**, 13 (1996).

[26] H. Gotoda, K. Maeda, T. Ueda, and R. K. Cheng, Combust. Flame **134**, 67 (2003).

[27] T. Schreiber and A. Schmitz, Phys. Rev. Lett. **77**, 635 (1996).

[28] D. Kugiumtzis, Phys. Rev. E **60**, 2808 (1999).

[29] T. Suzuki, T. Ikeguchi, and M. Suzuki, Phys. Rev. E **71**, 056708 (2005).

[30] S. Ramdani, F. Bouchara, and J. F. Casties, Phys. Rev. E **76**, 036204 (2007).

[31] Y. Hirata and K. Aihara, Phys. Rev. E **82**, 036209 (2010).

[32] K. Hayashi, H. Gotoda, and P. L. Gentili, Chaos **26**, 053102 (2016).

[33] P. J. Weck, D. A. Schaffner, M. R. Brown, and R. T. Wicks, Phys. Rev. E **91**, 023101 (2015).

[34] N. Marwan, J. F. Donges, Y. Zou, R. V. Donner, and J. Kurths, Phys. Lett. A **373**, 4246 (2009).

[35] R. V. Donner, Y. Zou, J. F. Donges, N. Marwan, and J. Kurths, Phys. Rev. E **81**, 015101 (2010).

[36] A. M. Fraser and H. L. Swinney, Phys. Rev. A **33**, 1134 (1986).

[37] K. Takagi and H. Gotoda, Bulletin of the American Physical Society (APS), 69th Annual Meeting of the APS Division of Fluid Dynamics, Vol. 61 (2016).

[38] Y. Tang, A. Zhao, Y. Y. Ren, F. X. Dou, and N. D. Jin, Physica A **449**, 324 (2016).

[39] M. Cencini, M. Falcioni, E. Olbrich, H. Kantz, and A. Vulpiani, Phys. Rev. E **62**, 427 (2000).

[40] Q. L. Li and Z. T. Fu, Phys. Rev. E **89**, 012905 (2014).

[41] C. S. Daw, J. F. Thomas, G. A. Richards, and L. L. Narayanaswami, Chaos **5**, 662 (1995).

[42] S. Datta, S. Mondal, A. Mukhopadhyay, D. Sanyal, and S. Sen, Combust. Theory Model. **13**, 17 (2009).

[43] S. Mondal, A. Mukhopadhyay, and S. Sen, Combust. Sci. Technol. **186**, 139 (2014).

[44] H. Gotoda, H. Nikimoto, T. Miyano, and S. Tachibana, Chaos **21**, 013124 (2011).

[45] L. Kabiraj, A. Saurabh, P. Wahi, and R. I. Sujith, Chaos **22**, 023129 (2012).

[46] K. Kashinath, I. C. Waugh, and M. P. Juniper, J. Fluid Mech. **761**, 399 (2014).

[47] H. Gotoda, Y. Shinoda, M. Kobayashi, Y. Okuno, and S. Tachibana, Phys. Rev. E **89**, 022910 (2014).

[48] H. Gotoda, Y. Okuno, K. Hayashi, and S. Tachibana, Phys. Rev. E **92**, 052906 (2015).

[49] L. Kabiraj, A. Saurabh, N. Karimi, A. Sailor, E. Mastorakos, A. P. Dowling, and C. O. Paschereit, Chaos **25**, 023101 (2015).

[50] S. Balusamy, L. K. B. Li, Z. Han, M. P. Juniper, and S. Hochgreb, Proc. Combust. Inst. **35**, 3229 (2015).

[51] T. Kamiński, M. Wendeker, K. Urbanowicz, and G. Litak, Chaos **14**, 461 (2004).

[52] A. K. Sen, G. Litak, T. Kamiński, and M. Wendeker, Chaos **18**, 033115 (2008).

[53] P. L. Curto-Risso, A. Medina, A. C. Hernández, L. Guzmán-Vargas, and F. Angulo-Brown, Physica A **389**, 5662 (2010).

[54] L. Yang, S. Ding, G. Litak, E. Song, and X. Ma, Chaos **25**, 013105 (2015).

[55] H. D. Ng, A. J. Higgins, C. B. Kiyanda, M. I. Radulescu, J. H. S. Lee, K. R. Bates, and N. Nikiforakis, Combust. Theory Model. **9**, 159 (2005).

[56] H. A. Abderrahmane, F. Paquet, and H. D. Ng, Combust. Theory Model. **15**, 205 (2011).

[57] A. R. Kasimov, L. M. Faria, and R. R. Rosales, Phys. Rev. Lett. **110**, 104104 (2013).